Electronic Supplementary Material (ESI) for Physical Chemistry Chemical Physics.

Supplementary Information

Electron-stimulated reactions in nanoscale water films adsorbed on α-Al_2O_3(0001)

Nikolay G. Petrik* and Greg A. Kimmel*

Physical Sciences Division, Pacific Northwest National Laboratory, MSIN K8-88, P.O. Box 999, Richland, WA 99352, USA.

*Corresponding authors. Email addresses – nikolai.petrik@pnnl.gov; gregory.kimmel@pnnl.gov

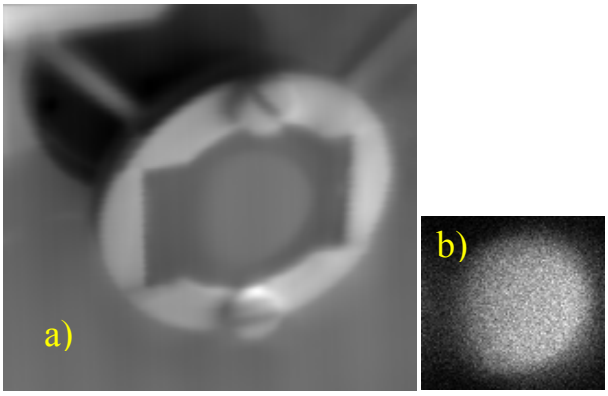

Fig. S1. a) Secondary electron image of a 40 ML H_2O film adsorbed on the Al_2O_3(0001) sample (mounted on the sample holder). The image is obtained by rastering a 500 eV electron beam over the sample (at 30 K) and collecting the emitted secondary electrons versus the beam X-Y deflection. The 10×10×1 mm crystal is attached to the resistively-heated ∅15 mm and 1 mm thick Ta base plate using high-temperature Aremco 865 cement adhesive and covered from the front with a Mo retaining ring and 2 Mo screws (seen in the image). The 7 mm diameter 40 ML thick water spot dosed on the Al_2O_3 surface with a molecular beam is also seen in this image (lighter grey). The good resolution of the image, especially for the water spot, indicates that charging is not a significant issue here. A K-type thermocouple is spot-welded to the back side of the Ta base plate (not seen here). The Ta resistive heating leads are seen in the upper left and right corners. b) O_2 ESD image from a 40 ML thick water spot dosed on the Al_2O_3 surface obtained by rastering

the 100 eV electron beam over the sample and measuring the O_2 signal versus the beam X-Y deflection. The electron beam is smaller than the molecular beam spot size on the sample (~1.5 mm and 7.0 mm, respectively). The ESD signals presented in this study are an average of 80,000 data points (400 pixels/scan × 200 points/pixel) per each 0.4 s scan.

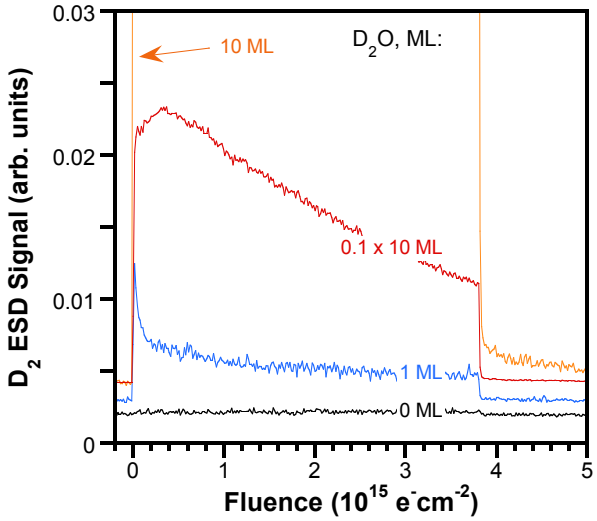

Fig. S2. D_2 ESD signals at 100 K versus electron fluence from 0, 1 and 10 ML of D_2O on Al_2O_3(0001). The traces are displaced for the sake of comparison. Radiation-induced change in the D_2 background signal is not significant (0 ML, black trace).

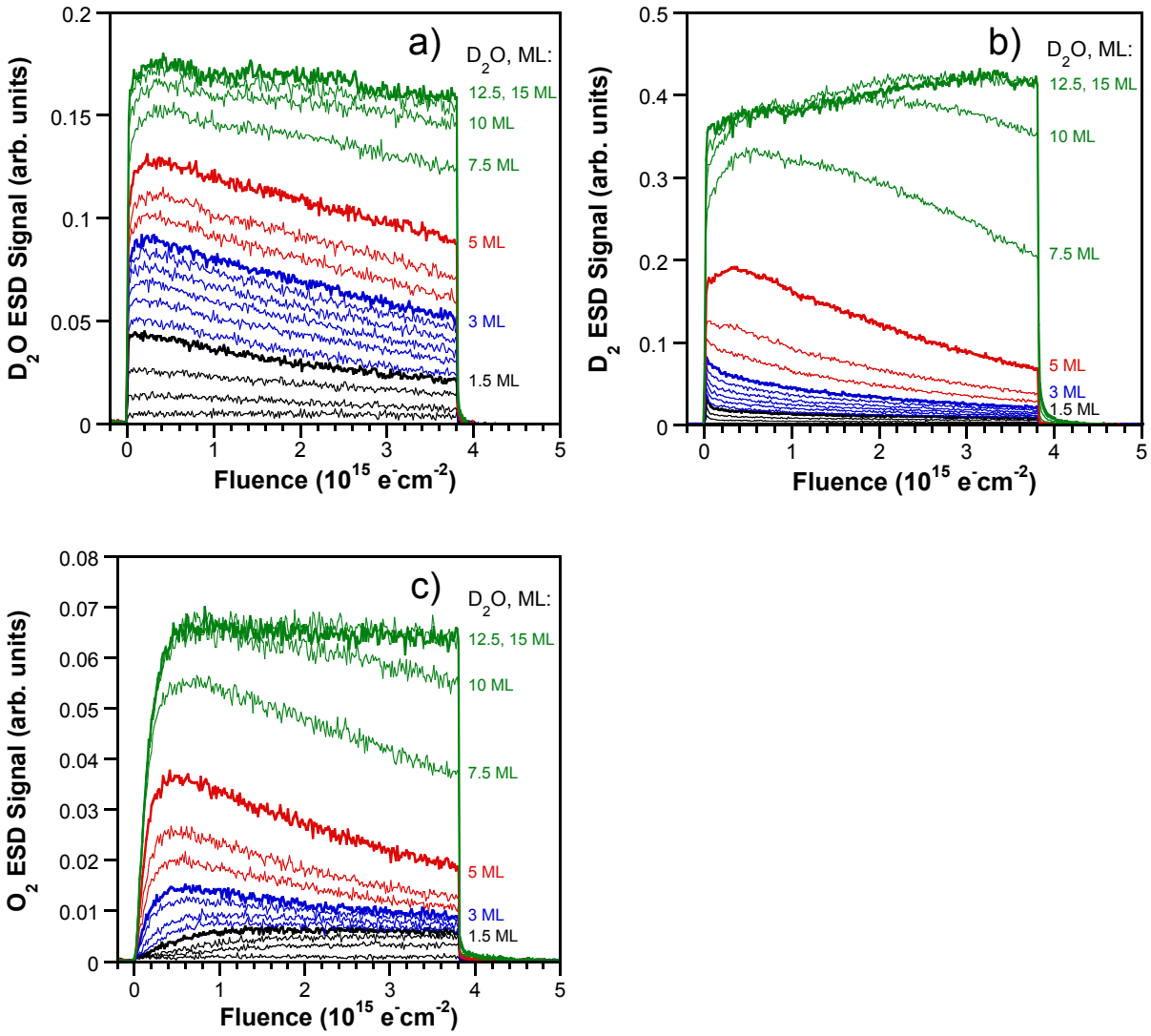

Fig. S3. D_2O, D_2 and O_2 ESD signals at 100 K versus electron fluence for various coverages of D_2O on $Al_2O_3(0001)$. (1 ML = 10^{15} cm^{-2}).

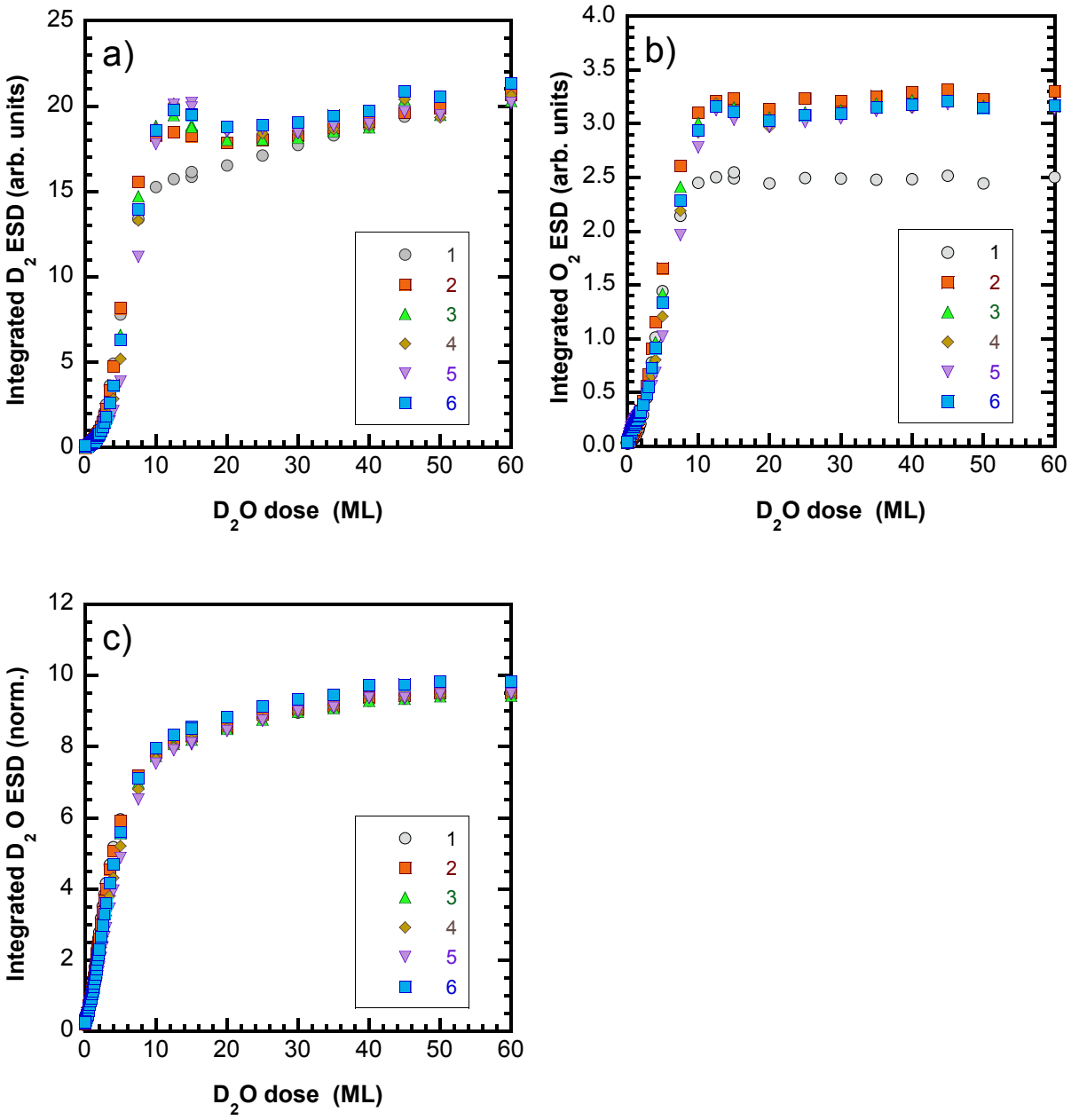

Fig. S4. a) D_2, b) O_2 and c) D_2O ESD yields integrated in different electron fluence ranges versus initial D_2O coverage on $Al_2O_3(0001)$ for the data presented in Fig. 3. The integrations start at ϕ_e = (1) 0, (2) 0.46, (3) 1.22, (4) 1.98, and (5) 2.74×10^{15} cm^{-2}, and the same integration width ($\Delta\phi_e = 0.76 \times 10^{15}$ cm^{-2}) is used for each. (6) The total ESD integrals from Fig. 3, arbitrarily scaled to facilitate comparison, are also shown. The initial D_2 ESD integral ((a),1, grey circles) is also multiplied by 0.9 for the sake of comparison. A small peak in D_2 ESD data (a) in the 8 – 20 ML coverage range, which is initially absent, develops at higher

fluences. This peak is associated with D_2 molecules produced at the Al_2O_3/D_2O interface from precursors accumulating on the alumina surface with irradiation time. A similar peak can be seen in the O_2 ESD data (b), but not in the D_2O ESD data (c). D_2O ESD occurs from the D_2O/vacuum interface and it is not associated with reactions at the Al_2O_3/D_2O interface.[1] O_2 is also produced at the D_2O/vacuum interface but it is correlated with D_2 production and associated with reactions at the Al_2O_3/D_2O interface (see more details in our earlier publications[2, 3]).

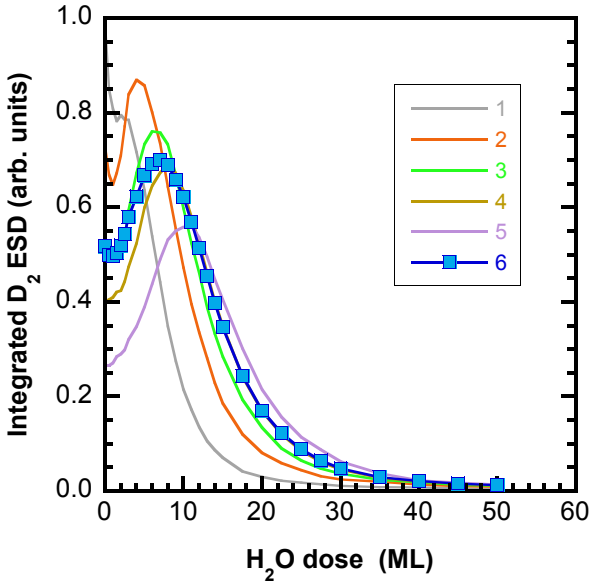

Fig. S5. D_2 ESD yields integrated in different electron fluence ranges versus the initial H_2O cap coverage in isotopically layered D_2O/H_2O films on $Al_2O_3(0001)$ for the data presented in Fig. 5. The integrations start at ϕ_e = (1) 0, (2) 0.30, (3) 1.07, (4) 1.83, and (5) 3.36 $\times 10^{15}$ cm^{-2} and the same integration width ($\Delta\phi_e$ = 0.30 $\times 10^{15}$ cm^{-2}) is used for each. (6) The total ESD integral from Fig. 5, arbitrarily scaled to facilitate comparison, is also shown. At higher fluence, the maximum in the D_2 ESD shifts to the higher H_2O coverage due to the film sputtering (initial coverage is higher than the actual one) and due to the greater contribution of the reactions at the Al_2O_3/D_2O interface.

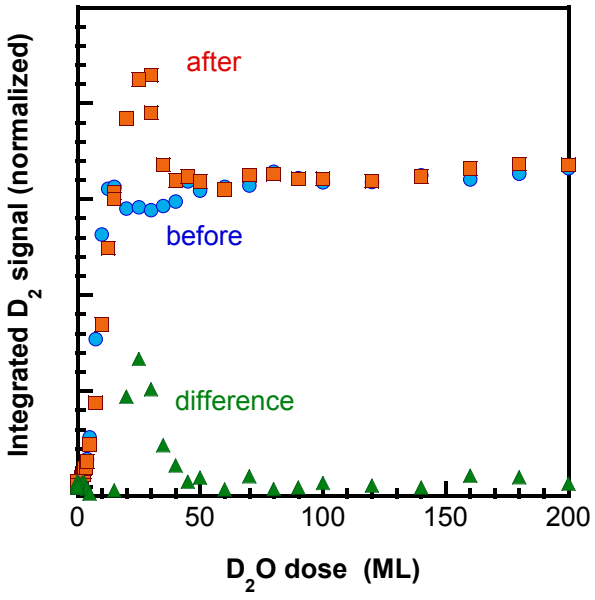

Fig. S6. Integrated D_2 ESD yields versus initial D_2O coverage on Al_2O_3(0001). The ESD yields are integrated during 1 s before the end of irradiation with a fluence of 3.8×10^{15} cm^{-2} (blue circles) and 20 s after the end of irradiation (red squares). The maximum in the D_2 ESD signal near 25 ML observed after irradiation is due to D_2 molecules produced at the Al_2O_3/D_2O interface and diffusing through the film to desorb. Above 25 ML, this signal decreases since the D_2 yield at the Al_2O_3/D_2O interface decreases with coverage (compare to the Fig. 5b and note that the actual coverage of the film is lower than initial due to sputtering). Above 50 ML, the post-radiation D_2 ESD yield stabilizes at a coverage-independent level proportional to the D_2 ESD signal at the end of irradiation (blue circles) and associated with a certain pumping out rate of our chamber. This component of the signal is associated mainly with the electron-induced processes at the D_2O/vacuum interface. Signal normalization and subtraction of this "pumping tail" yields the D_2 component produced at the Al_2O_3/D_2O interface (green triangles). Similar post-irradiation sample outgassing was also observed earlier for the Pt(111)/ASW systems and associated with the molecular hydrogen produced at the metal/water interface.[4, 5]

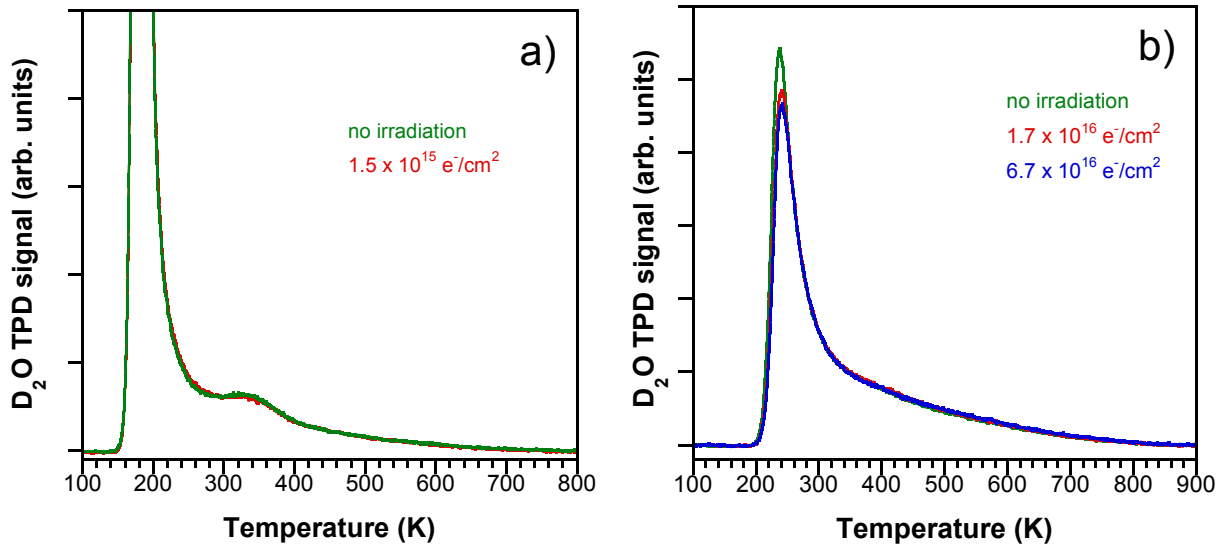

Fig. S7. a) TPD spectrum of 5 ML D_2O irradiated with 1.5×10^{15} e^-/cm^2 electrons (E_i = 100 eV) (red) and of similar coverage of non-irradiated D_2O (green). b) TPD spectrum of 0.5 ML D_2O dosed on $Al_2O_3(0001)$ pre-irradiated with 500 eV electrons (1.7×10^{16} e^-/cm^2 and 6.7×10^{16} e^-/cm^2) and not irradiated (red, blue and green respectively). 1 ML = 10^{15} cm^{-2}.

References

1. N. G. Petrik and G. A. Kimmel, *J. Chem. Phys.*, 2005, **123**, 054702.
2. N. G. Petrik, A. G. Kavetsky and G. A. Kimmel, *J. Phys. Chem. B*, 2006, **110**, 2723-2731.
3. N. G. Petrik, A. G. Kavetsky and G. A. Kimmel, *J. Chem. Phys.*, 2006, **125**, 124702.
4. N. G. Petrik and G. A. Kimmel, *J. Chem. Phys.*, 2004, **121**, 3736 - 3744.
5. N. G. Petrik and G. A. Kimmel, *Phys. Rev. Lett.*, 2003, **90**, 166102.